Vol 18 No 10, October 2009
1674-1056/2009/18(10)/4547–05

Chinese Physics B

© 2009 Chin. Phys. Soc.
and IOP Publishing Ltd

Enhanced field emission characteristics of thin-Au-coated nano-sheet carbon films

Gu Guang-Rui(顾广瑞)[a)†] and Ito Toshimichi(伊藤利道)[b)]

[a)] *Department of Physics, College of Science, Yanbian University, Yanji 133002, China*
[b)] *Division of Electrical, Electronic and Information Engineering, Graduate School of Engineering, Osaka University, Osaka 565-0871, Japan*

(Received 30 January 2009; revised manuscript received 23 March 2009)

This paper reports that the nano-sheet carbon films (NSCFs) were fabricated on Si wafer chips with hydrogen–methane gas mixture by means of quartz-tube-type microwave plasma chemical vapour deposition (MWPCVD). In order to further improve the field emission (FE) characteristics, a 5-nm Au film was prepared on the samples by using electron beam evaporation. The FE properties were obviously improved due to depositing Au thin film on NSCFs. The FE current density at a macroscopic electric field, E, of 9 V/μm was increased from 12.4 mA/cm^2 to 27.2 mA/cm^2 and the threshold field was decreased from 2.6 V/μm to 2.0 V/μm for Au-coated carbon films. A modified F-N model considering statistic effects of FE tip structures in the low E region and a space-charge-limited-current effect in the high E region were applied successfully to explain the FE data of the Au-coated NSCF.

Keywords: nano-sheet carbon films, field emission, microwave plasma chemical vapour deposition, space-charge-limited-current

PACC: 7970, 6146

1. Introduction

In recent years, a great effort has been made to develop of electron field emitters for the application in display products.[1−3] Much attention has been paid to carbon-based emitters which have good electron field emission (FE) properties such as relatively low threshold electric fields[4] and high FE current densities.[5] Many reports indicate that amorphous carbon films are also promising candidates for the field emitters due to their unique chemical, electrical, optical, and mechanical properties.[6] In order to obtain such FE properties as low threshold voltages and high current densities, it may be essential to fabricate nano-structured carbon films. Thus recently various nano-structured carbon films have been investigated. Zhang *et al* [7] reported that the low threshold field of carbon nanotubes was attributed to a random distribution which brought a high geometric enhancement factor. Wang and co-workers found that the good FE properties of carbon nano-sheets[8] and carbon nanoflakes[9] might be due to the high density of graphite edges with potential emission sites. The research results given by Wang *et al* [10] indicated that the carbon nanocones with a large aspect ratio had a higher FE current and a lower threshold field. The FE properties of other nano-carbon films have also been studied.[11] So far, we have reported that high FE current densities can be obtained from nano-sheets and nano-needles carbon films.[12,13]

All kinds of carbon nanostructured films have good FE properties, however, it is difficult to more improve their FE properties. The surface treatment may be an effective method to enhance the FE properties of carbon nanostructured films. Kung *et al*[14] reported that the emission current of the carbon nanotube arrays treated by oxygen and ozone was increased. An effective method by low energy carbonhydrogen ion treatment to enhance field emission of the carbon nanotubes is demonstrated by Li *et al.*[15] The FE properties of carbon nanostructured films coated by a thin metal film may be able to be improved due to surface modification, and the investigation on this has been not reported at present. So we fabricated nano-sheet carbon films (NSCFs) on Si substrates by means of the quartz-tube-type MWPCVD and subsequently deposited a 5-nm Au film on the NSCFs by using an electron beam (EB) evaporation method, and the FE characteristics of Au-coated NSCFs were studied in this study.

†Corresponding author. E-mail: grgu@ybu.edu.cn

2. Experimental

First, chemically cleaned single-crystalline Si substrates were ultrasonically scratched with diamond powders. (Such a treatment is commonly employed as a standard nucleation enhancement method for polycrystalline diamond chemical vapor deposition (CVD) growth on a Si substrate.[16]) Furthermore, the Si substrate surfaces were additionally pretreated for 10 min using H_2 plasma created with 300 W microwave power at 4×10^3 Pa. Then, carbon films were deposited at a total pressure of 8×10^3 Pa for 2 h on the Si substrates thus prepared by means of the quartz-type MWPCVD method with a mixture of 5-sccm CH_4 and 20-sccm H_2 gases at 450-W power of 2.45-GHz microwave. The base pressure of the CVD chamber employed was below 1.3×10^{-4} Pa. Finally, an about 5-nm Au film was deposited on the carbon films by using EB evaporation.

Surface morphologies of the carbon films before the metal deposition were observed with an FE scanning electron microscope (FESEM) while the structures of the carbon films were characterized with Raman spectroscopy. The FE measurements were performed at room temperature (RT) below 6.6×10^{-4} Pa in another high vacuum chamber. A sample with an FE area of about 2×5 mm^2 acted as a cathode while an aluminum plate was utilized as its counter anode. The anode was set to be 100 μm away from the sample surface by using two 50-μm Teflon sheets as a spacer. Macroscopic average electric fields ranging from 0 to 9 V/μm were applied between the anode and the cathode.

3. Results and discussion

As shown in Fig.1, Raman spectra taken from a typical carbon film uncoated with Au thin film have two Raman peaks located at about 1353 cm^{-1} and 1587 cm^{-1} respectively, indicating that standard features are formed in the carbon films.

A typical FESEM image of a typical carbon film uncoated with Au thin film is shown in Fig.2(a). This picture indicates that the film surface is composed mainly of stand-up nano-structured carbon sheets which are complicatedly twisted with each other. This kind of structure is a little different from that of other nano-sheets.[8] The SEM image looks like veins with about 100-nm in width and 1-μm in length. Moreover, many nano-protuberances are observed on the surface of nano-sheets, so a large numbers of potential field emission sites can be expected to be formed on the nano-carbon films.[8] The formation of the carbon nano-sheets can be attributed to higher CH_4 concentration and substrate temperature. Higher CH_4 concentration and substrate temperature offer the driving force for nanosheet growth.[17] A high flux of fast atoms and ions bombardment associated with the inductively coupled microwave plasma will yield growth along the strongly bonded planes of graphite sheets, rather than in the more weakly bonded stacking direction.

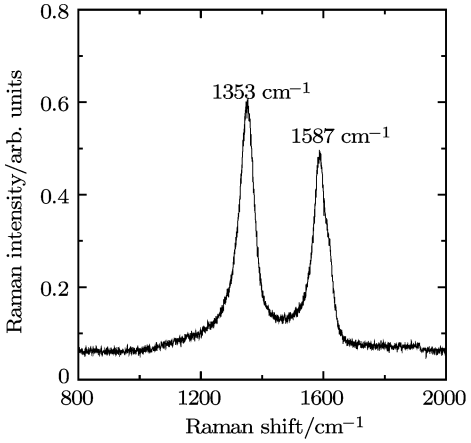
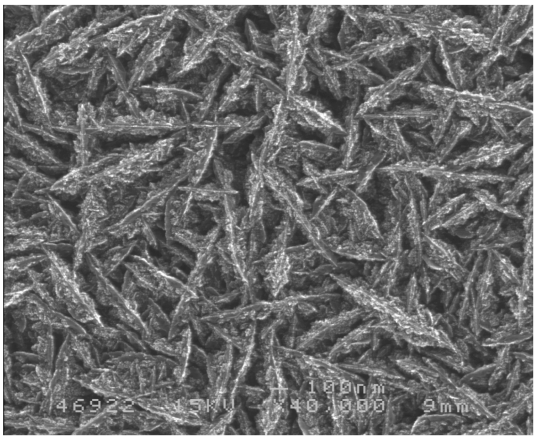


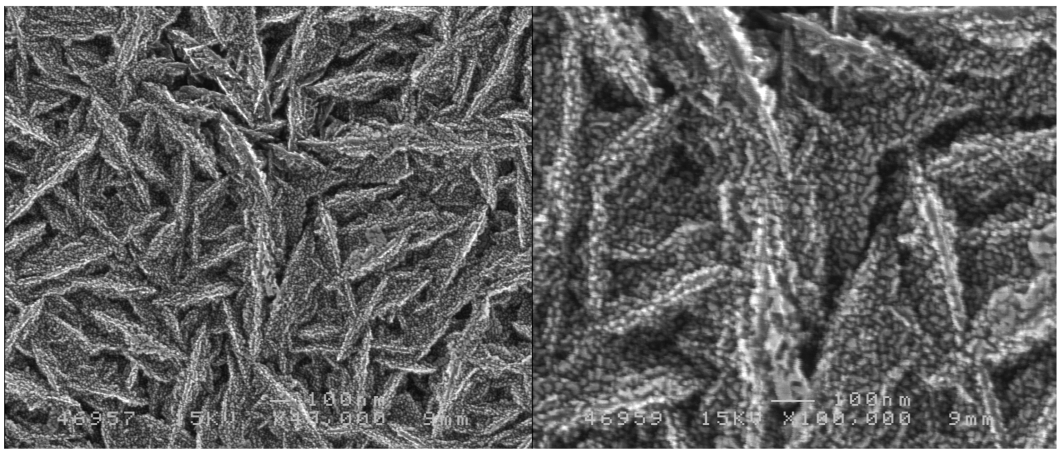
Fig.1. Typical Raman spectrum taken from a typical as-deposited carbon film (with no metal film) fabricated in the present study.

The 5-nm Au-coated carbon films and its corresponding magnifications are shown in Figs.2(b) and 2(c), respectively. These two images show that large numbers of about 10-nm particles are formed on the Au-coated carbon film. The formation of nano-sized Au particles may be attributed to a self-assembly process due to little reactivity between the Au atoms and the carbon atoms.

In this study, the threshold E was defined as E at which the emission current density, J of 1 μA/cm^2 appeared.[4] Figure 3 shows FE current density versus macroscopic electric field (J–E) data of the NSCF coated without and with 5-nm Au film. As shown in Fig.3, the as-deposited NSCF exhibits good emission properties. The threshold is 2.6 V/μm and the current density is 12.4 mA/cm^2 at the field of 9 V/μm. After Au deposition, the sample exhibits enhanced FE properties than the as-deposited NSCF, with the lower threshold field of 2.0 V/μm and larger emission current density of 27.2 mA/cm^2 at the field of 9 V/μm.



(a)



(b) (c)

Fig.2. The FESEM images taken from nano-structured carbon films coated (a) without Au films, (b) with 5-nm Au films and (c) a corresponding magnification of (b).

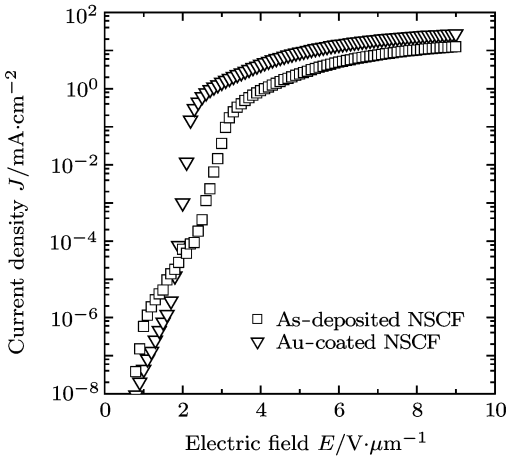


Fig.3. The FE current density J versus macroscopic electric field E of typical FE characteristics obtained from the nano-sheet carbon films coated with and without the Au films shown in Fig.2.

The increase of the emission properties of Au-coated NSCFs may be contributed to nano-particles' formation on its surface, because the formation of nano-particles can induce the increase of potential FE sites. In addition, figure 3 shows that the FE current density of Au-coated carbon films steeply increases with increasing E below the E of 2.5 V/μm, above which there is an obvious saturation behavior of J. It is shown that the saturation behavior of J happens at the lower E for the Au-coated NSCF than those for the as-deposited NSCF.

In order to fully understand the FE mechanism concerned, the FE data of samples should be discussed separately in the low and high E regions. In the unsaturated J region or in the low E region, a modified F–N model considering the statistical distribution in structure of the FE tips and E-dependent parameters gives the following relation between J in A/m^2 and E in V/m:[12,13]

$$\ln \frac{J}{E^2} \approx \ln \left(\frac{1.54 \times 10^{-6} S_r \beta^2}{\varphi} \right) - \frac{6.83 \times 10^9 \varphi^{3/2}}{\beta} \left(\frac{1}{E} \right), \quad (1)$$

where S_r is an effective relative emission area, β is an effective field enhancement factor, and φ is the work function of the tip material in eV.

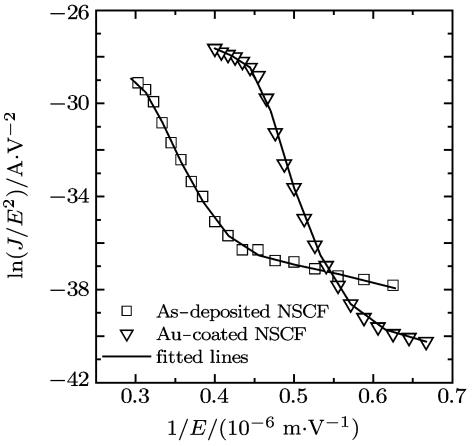


Fig.4. The F–N plots in the unsaturated field emission current region with a set of short lines fitted using a local fitting method with E-dependent parameters of the effective field enhancement factor and the effective relative emission area.

Here, the work function φ is assumed to have a constant value of 4.5 eV and 5.1 eV for the as-deposited NSCF and Au-coated NSCF, respectively. S_r and β are assumed to change with E while they are regarded as constant values in each E sector of about 0.1 V/μm. Figure 4 shows the observed J–E data of samples in the unsaturated J region and those fitted in every sequential 0.1-V/μm E region by using a local fitting method,[12,13] indicating that the modified F–N model can reasonably well reproduce the experimental data.

The fitting parameters S_r and β deduced as a function of E in the E region from 1.4 V/μm to 3.5 V/μm are shown in Figs.5(a) and 5(b), respectively. For two samples examined, the β descends with increasing E in the low E region and then tends to be saturated to their minimum values in the high E region (Fig.5(a)), this is coincident with our prevenient result.[12,13] The maximum β value of the Au-coated NSCF is larger than the as-dopesited NSCF, this may be attributed to the formation of nano-Au particles on the surface of the carbon sheets which can lead to the descending of the curvature radius of FE sites. This is a possible reason that the threshold field of the Au-coate NSCF is lower than that of the as-deposited NSCF.

As shown in Fig.5(b), the S_r increases with increasing E in the low E region and then tends to be saturated to their maximum values in the high E region, this is coincident with our prevenient result, too.[12,13] However, the effective emission area of the Au-coated NSCF was extremely larger than that of the as-deposited NSCF, this may be due to a large number of nano-Au particles formed on the surface of the carbon sheets. A large number of nano-Au particles cause the increase of the total effective FE area of the emitter, so the FE current density of the Au-coate NSCF is higher than that of the as-deposited NSCF.

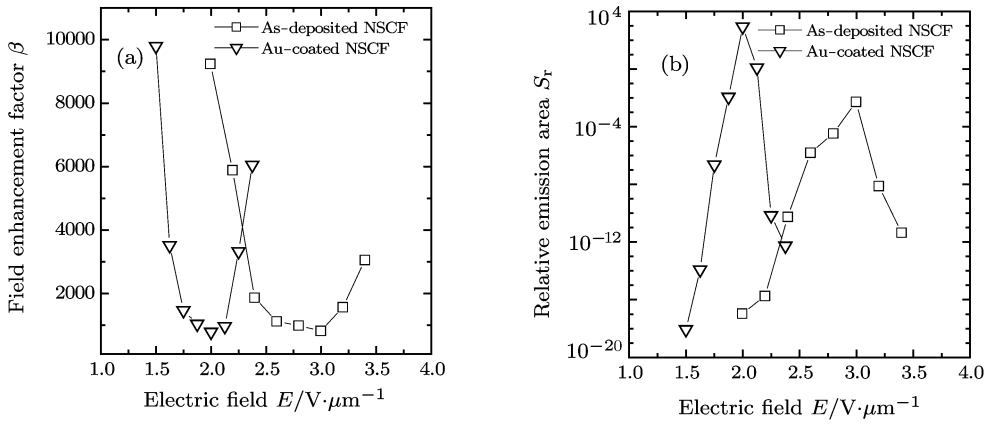


Fig.5. Fitting parameters of (a) the effective field enhancement factor β and (b) the effective relative emission area S_r, deduced from the local fitting procedure with Eq.(1) in the text as a function of the macroscopic electric field E.

The change of the effective field enhancement factor and the relative emission area with increasing E is consistent with our prevenient reports and has been reasonably explained.[12,13] The FE behavior in J at sufficiently high E can be reasonably explained by using the space-charge-limited-current (SCLC) model represented in terms of the Child–Langmuir law[18] as follows:

$$J \propto E^{3/2}. \tag{2}$$

As shown in Fig.6, the measured FE data can be well fitted only above the E of 6.5 V/μm and 5.5 V/μm by using Eq.(2) for the as-deposited and Au-coated NSCF, respectively. This is a possible explanation that the saturation behavior in J of the Au-coated NSCF happened at the lower E than that of the as-deposited NSCF. Figure 6 shows that the SCLC model may be a strong candidate for the mechanism explaining the saturated behaviour observed at the high FE currents.

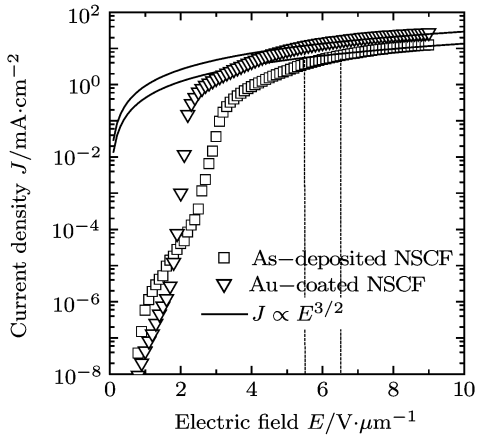


Fig.6. J–E data with a curve fitted as $J \propto E^{3/2}$ in terms of the Child–Langmuir space-charge-limited-current model.

4. Conclusion

The nano-sheet carbon films fabricated by means of a high-power MWPCVD method were coated with an above 5-nm Au film. The field emission characteristics of the Au-coated NSCF were obviously improved, in comparison with that of the as-deposited NSCFs. The FE current density at a macroscopic electric field of 9 V/μm was increased from 12.4 mA/cm^2 to 27.2 mA/cm^2 and the threshold field was decreased from 2.6 V/μm to 2.0 V/μm for Au-coated carbon films. The measured FE data in the unsaturated J region were interpreted by using a modified F–N model considering the statistic effects of the tip structure whereas those in the saturated J region were explained in terms of a space-charge-limited-current mechanism. The enhanced FE properties of the Au-coated NSCF were resulted in the bigger effective field enhancement factor and the extremely high effective emission area. The FE behavior in the saturated J region was found to be well reproduced in terms of the Child–Langmuir law following the relation $J \propto E^{3/2}$.

References

[1] Chen L, Zhang G M, Wang M S and Zhang Q F 2005 *Chin. Phys.* **14** 181

[2] Song J H, Zhang G M, Zhang Z X, Sun M Y and Xue Z Q 2004 *Acta Phys. Sin.* **53** 4392 (in Chinese)

[3] Ma Y P, Wang X F, Gu Z X, Li Z H, Wang M and Xu Y B 2007 *Acta Phys. Sin.* **56** 6701 (in Chinese)

[4] Li J J, Gu C Z, Wang Q, Xu P, Wang Z L, Xu Z and Bai X D 2005 *Appl. Phys. Lett.* **87** 143107

[5] Wang J, Teraji T and Ito T 2005 *Diamond Relat. Mater.* **14** 2074

[6] Mao D S, Wang X, Liu X H, Li Q and Xu J F 2000 *Diamond Relat. Mater.* **9** 1876

[7] Zhang Y B, Lau S P, Huang L and Tanemura M 2005 *Appl. Phys. Lett.* **86** 123115

[8] Wang J J, Zhu M Y, Outlaw R A, Zhao X, Manos D M, Holloway B C and Mammana V P 2004 *Appl. Phys. Lett.* **85** 1265

[9] Wang J J, Zhu M Y, Zhao X, Outlaw R A, Manos D M, Holloway B C, Park C, Anderson T and Mammana V P 2004 *J. Vac. Sci. Technol.* B **22** 1269

[10] Wang W H, Lin Y T and Kuo C T 2005 *Diamond Relat. Mater.* **14** 907

[11] Gu G R, Wu B J, Jin Z and Ito T 2008 *Chin. Phys.* B **17** 716

[12] Gu G R and Ito T 2008 *Diamond Relat. Mater.* **17** 817

[13] Gu G R, Jin Z and Ito T 2008 *Chin. Phys.* B **17** 1467

[14] Kung SC, Hwang K C and Lin I N 2002 *Appl. Phys. Lett.* **80** 4819

[15] Li N, Gong J, Zhu D and Zhu Z 2007 *Nucl. Sci. Tech.* **18** 276

[16] Jiang N, Nishimura K, Shintani Y and Hiraki A 2003 *J. Cryst. Growth* **255** 102

[17] Wang J J, Zhu M Y, Outlaw R A, Zhao X, Manos D M and Holloway B C 2004 *Carbon* **42** 2867

[18] Child C D 1911 *Phys. Rev.* **32** 492
Langmuir I 1921 *Phys. Rev.* **21** 419